BRIEF NOTES

Simultaneous concentration and velocity measurement inside a plane turbulent mixing layer(*)

J. L. BOUSGARBIES, A. COLLIN and J. NERAULT (POITIERS)

EXPERIMENTAL techniques were performed to study hydrodynamic and concentration fields inside a plane turbulent mixing layer. The fluids were water and the aqueous solution of a passive scalar, respectively, emerging with different velocities in a rectangular duct. At first, the coherent structures evolution was observed by means of flow visualization. Then, simultaneous measurement of the instantaneous velocity components of the flow and of the solute concentration were performed at several locations inside the mixing layer.

1. Introduction

I THE LITERATURE on the diffusion of a passive scalar across turbulent mixing layer zones, experiments are generally performed from gas flows, either with thermal contamination [1, 2] or in the case of a solute substance [3]. Also, some studies of mass transport between reactive liquid streams have been reported [4, 5, 6].

The present work is an attempt to investigate the turbulent structure and diffusive characteristics associated with the mixing between two uniform parallel flows. The streams
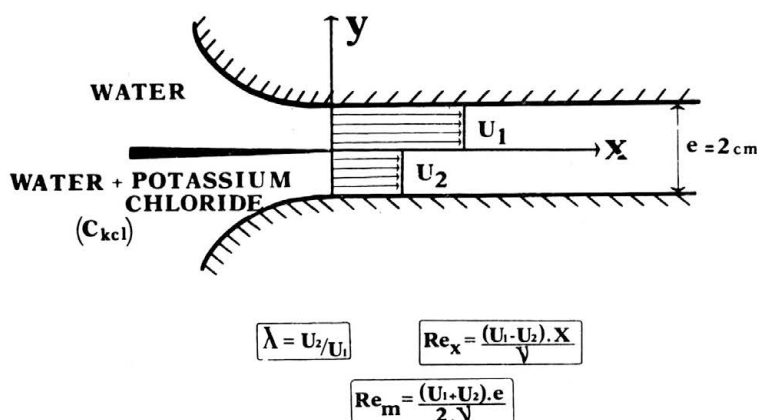

FIG. 1. Flow configuration.

which had equal thickness (1 cm) began to mix together downstream of the trailing edge of the splitter plate (Fig. 1). The test section was 25 cm long, 10 cm span and 2 cm high. The liquids flows were water and an aqueous solution of potassium chloride. In each experiment the water flow had the higher rate equal to 13 cm/s.

The flow pattern in the mixing layer could be observed when phenolphtalein was diluted in one stream. Sequences showing the appearance and growth of coherent structures were both filmed and recorded by photography and videoscopy. A laser beam and a set of optical lens allowed to obtain thin light sections of the flow.

Simultaneous measurements of the local values of the potassium chloride concentration and of the flow velocity components were performed by combining the conductivity and the two colours laser-Doppler anemometry. The sensitive part of a micro-conductivity probe was located downstream and near the intersection point of the laser beams. The characteristic length of the overall sampling volume was about 0.6 mm. Details of the micro-conductivity probe are presented in [7].

2. Results

2.1. Flow configuration

Examples of visualization are shown on the side view in Fig. 2. Flow is from left to rigth with the lower stream containing the phenolophtalein (white). Each picture exhibits the flow field from the trailing edge to the end of the test section. At once the interface between the coloured inner flow and undyed upper one is plane. Afterwards, small waves

$\lambda = 0.28$ $\Delta U/U_m = 1.1$ $R_{ex} = 410$ /cm $R_{em} = 740$

$\lambda = 0.31$ $\Delta U/U_m = 1.0$ $R_{ex} = 750$ /cm $R_{em} = 1400$

$\lambda = 0.4$ $\Delta U/U_m = 0.85$ $R_{ex} = 500$ /cm $R_{em} = 1150$

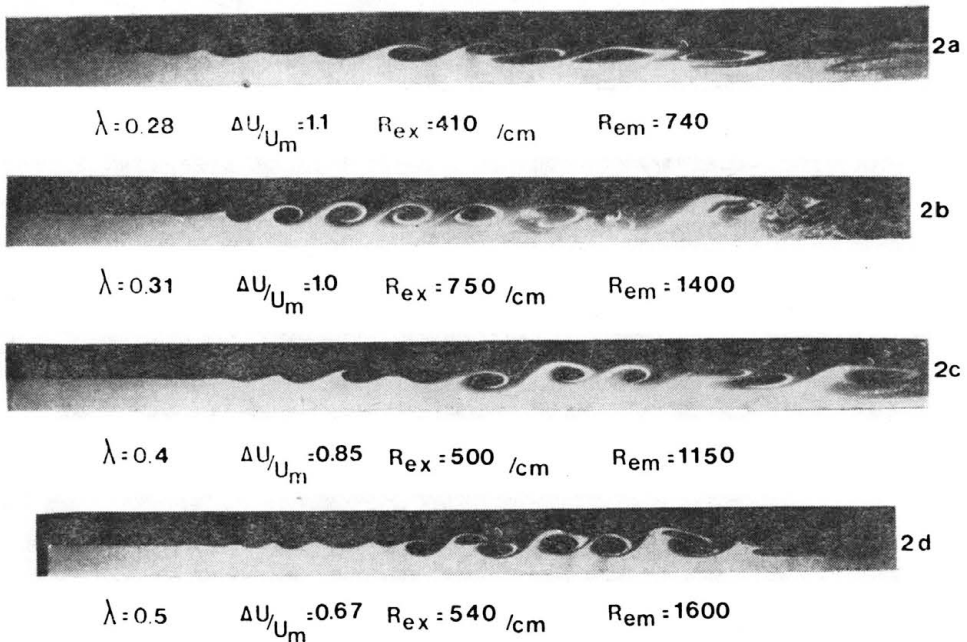$\lambda = 0.5$ $\Delta U/U_m = 0.67$ $R_{ex} = 540$ /cm $R_{em} = 1600$

Fig. 2. Side views of coherent structures.

appear, which grow up and give vortex structures. Far away, as reported by [8, 9, 10], the vortex pairing between two neighbouring structures is observed.

The two-dimensional aspect of the coherent structures in the upstream part of the mixing layer is clearly illustrated by the top view given in Fig. 3. Another interesting feature can be noted: downstream of two-dimensional vortex rolls, a spanwise disturbance
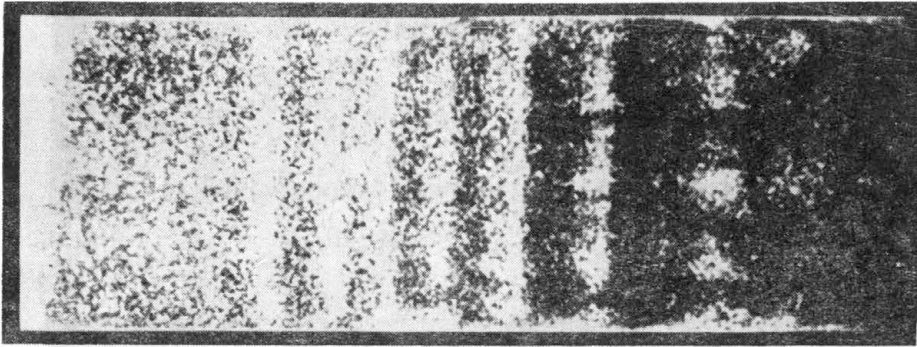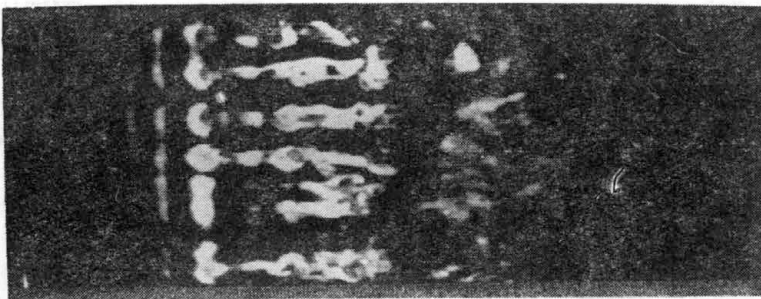

3a

$\lambda = 0.37$ $\Delta U/U_m = 0.91$ $R_{em} = 1000$ $R_{ex} = 460/cm$
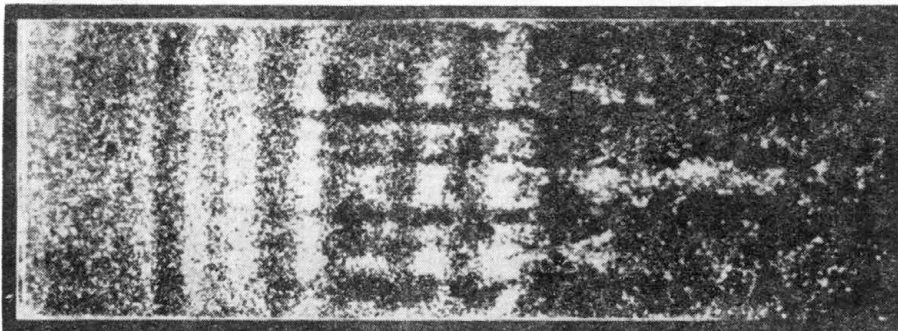
3b

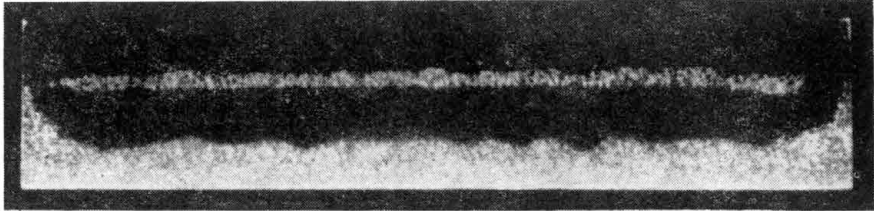$\lambda = 0.31$ $\Delta U/U_m = 1.06$ $R_{em} = 1550$ $R_{ex} = 820/cm$

3c

$\lambda = 0.15$ $\Delta U/U_m = 1.47$ $R_{em} = 1210$ $R_{ex} = 900/cm$

Fig. 3. Top views.

appears. This lateral ondulation increases downstream and gives longitudinal structures which can be observed particulary in Fig. 3c. This ondulated aspect, previously noted [12] and predicted [13], is evident on the transverse sections of the flow given in Fig. 4.

From a set of visualizations obtained with several velocity ratios, the position where the two-dimensional structures and the vortex pairing respectively appear, is referenced.
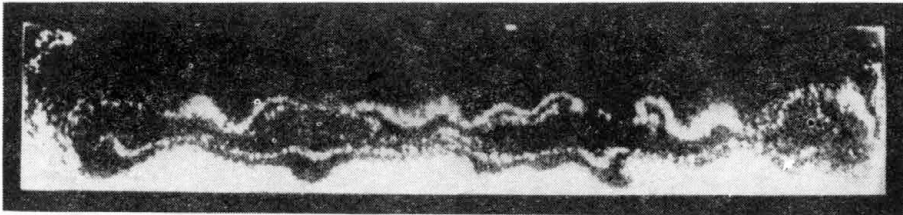
4a

$\lambda = 0.31$ $\Delta U/U_m = 1.0$ $R_{em} = 1550$ $R_{ex} = 7370$
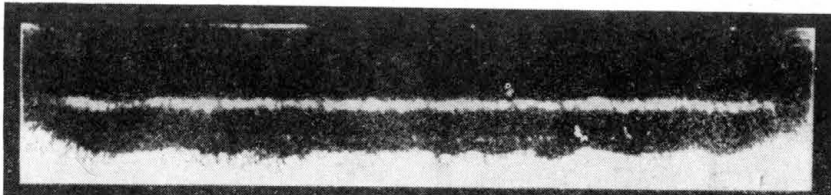
4b

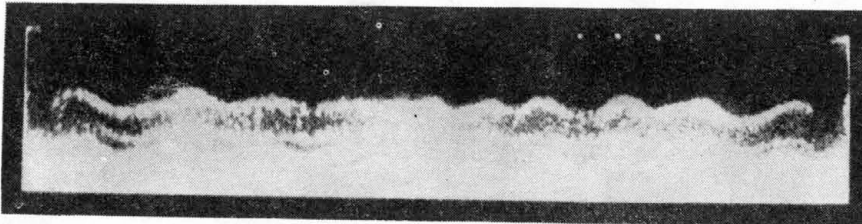$\lambda = 0.31$ $\Delta U/U_m = 1.0$ $R_{em} = 1550$ $R_{ex} = 11500$

4c

$\lambda = 0.23$ $\Delta U/U_m = 1.25$ $R_{em} = 1500$ $R_{ex} = 6400$

4d

$\lambda = 0.23$ $\Delta U/U_m = 1.25$ $R_{em} = 1500$ $R_{ex} = 8200$

FIG. 4. Transverse views showing ondulations.

The corresponding X coordinates, denoted by X_S and X_A, respectively, are increasing functions of the velocity ratio as it is shown in Fig. 5. Then, when the velocity difference of the two initial streams is small (i.e. $\lambda = 1$), the observations of coherent structures requires a longer test section.
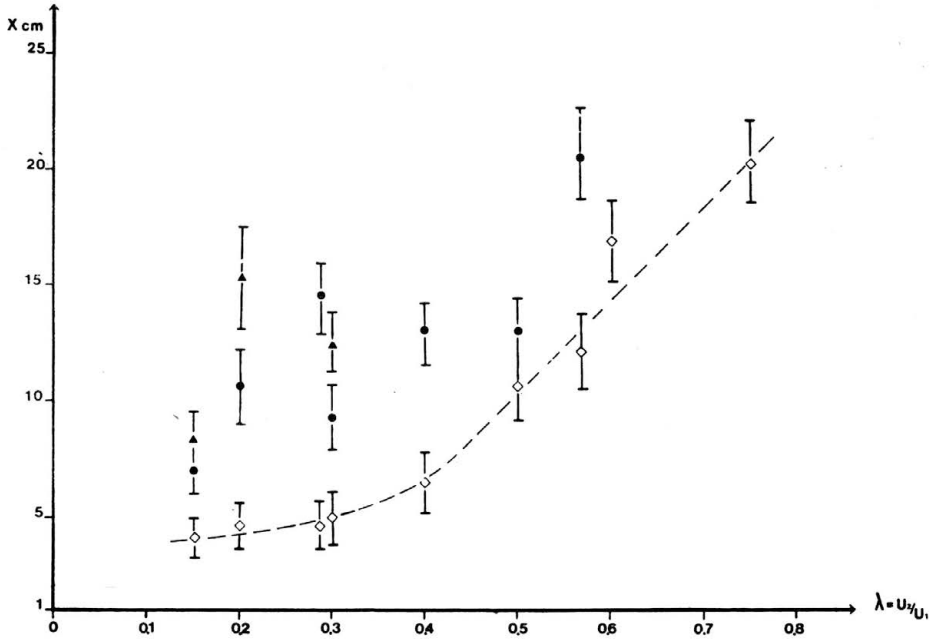

Fig. 5. Variation of the coordinate of the structure appearance ◇, vortex pairing ●, and vortex breakup ▲ with the velocity ratio.

2.2. Velocity and concentration fields

Instantaneous voltages coming from velocimeters counters and a conductimeter were recorded. From a set of data the time average values and the fluctuating values of the velocity component as well as the solute concentration were computed.
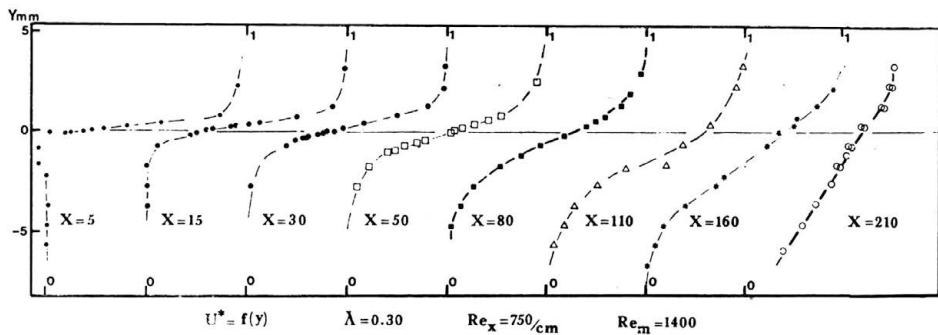

Fig. 6. Mean longitudinal velocity profiles.

Examples of mean longitudinal velocity and concentration profiles, obtained when the λ parameter was 0.3, are given in Figs. 6 and 7 respectively. The reduced velocity and concentration values are expressed by the relation:

$$U^*(x, y) = \frac{\bar{u}(x, y) - U_2}{U_1 - U_2},$$

$$\tilde{C}(x, y) = \frac{\bar{c}(x, y)}{C_2},$$

where C_2 denotes the concentration value in the potassium chloride stream, outside the mixing layer.
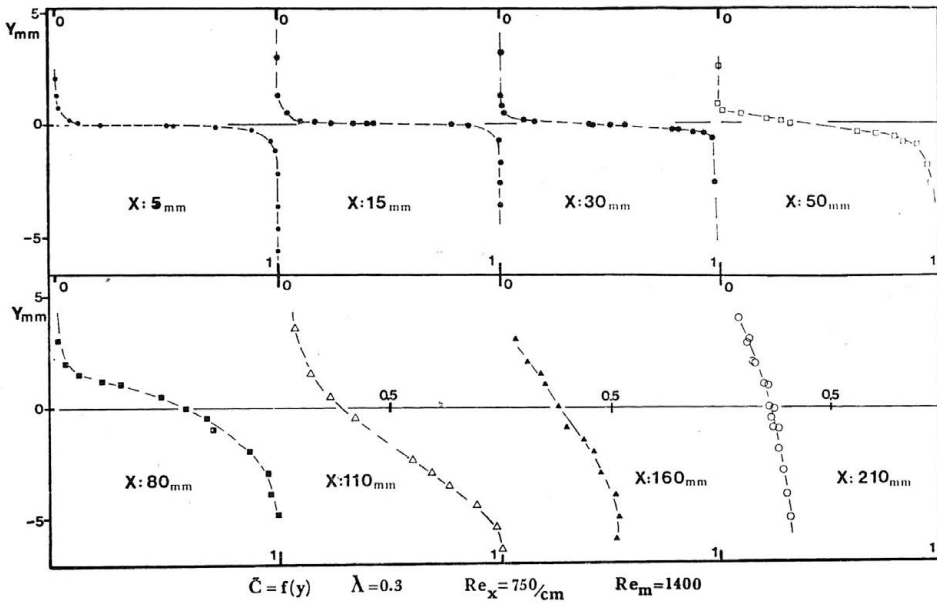

FIG. 7. Concentration profiles.

As it is well known for the velocity field, the concentration distribution is self-similar in the upstream part of the mixing layer, Fig. 8. The reference length used to calculate the dimensionless coordinate $\tilde{y}$ is the concentration layer thickness. Beyond $X = 11$ cm, the reduced concentration c never reaches unity in a transverse section; this means that the mixing takes place in the whole of the test section. This high level mixing corresponds to the breakup of the vortex rolls which can be seen in the vicinity of the lower wall (Fig. 3b — $\lambda = 0.3$).

In Figs. 9 and 10 are plotted, for three velocity ratios, the maximum of the velocity and the concentration fluctuations intensity in a transverse section as a function of the X coordinate. The more important concentration fluctuations are located in the region where the pairing vortex has been revealed by the visualization. On the other hand, the higher velocity fluctuations are recorded downstream, in the zone where the vortex breakup has been observed.
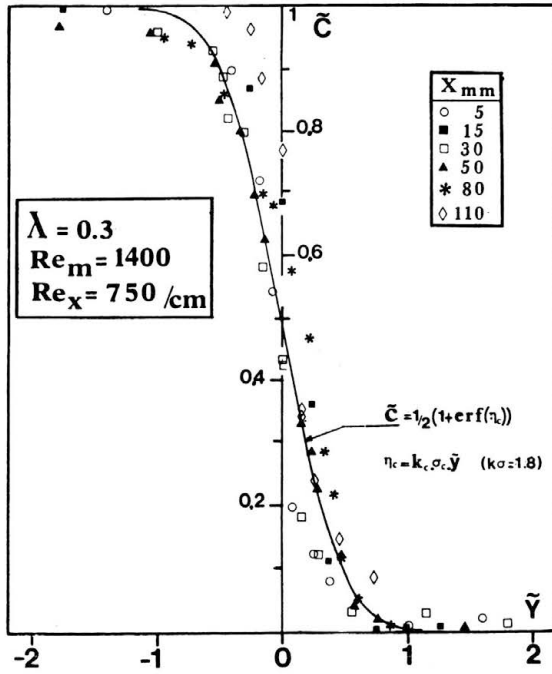
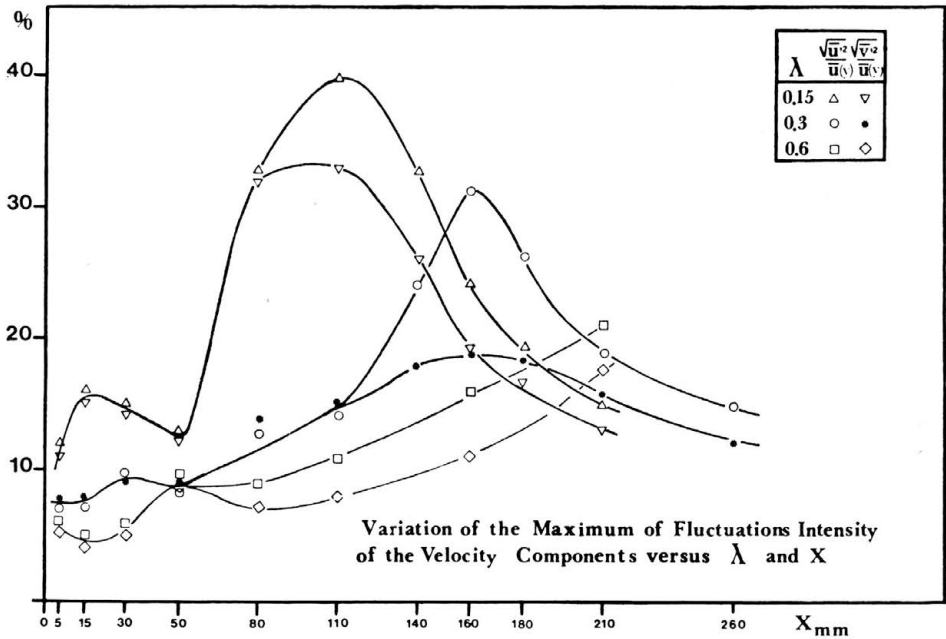FIG. 8. Dimensionless concentration distribution.

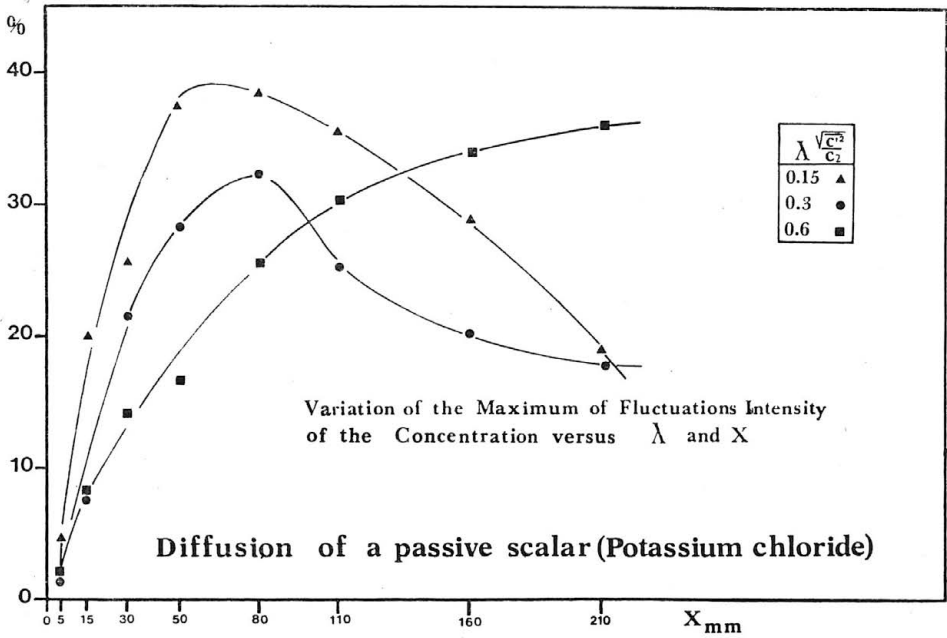FIG. 9. Variation of the maximum of the velocity fluctuations intensity with X.

FIG. 10. Variation of the maximum of the concentration fluctuations intensity with X.

The distributions of the longitudinal and transverse velocity concentration correlation coefficients are presented in Figs. 11 and 12. It is of interest to note that these normalized velocity and concentration correlations never achieve magnitudes greater than 60%. In the case reported here ($\lambda = 0.3$), the maximum correlations are recorded between 8 and 11 cm from the trailing edge of the splitter plate; that is, the part of the test section where
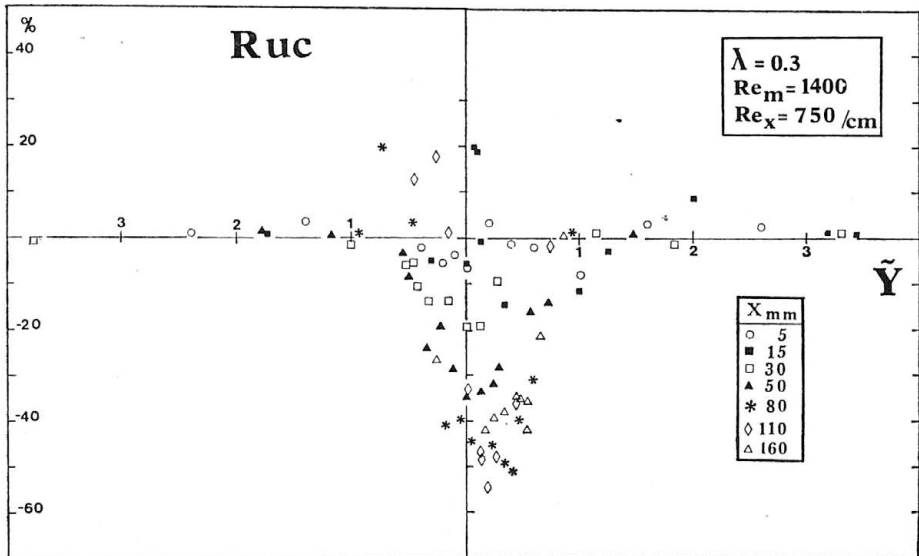

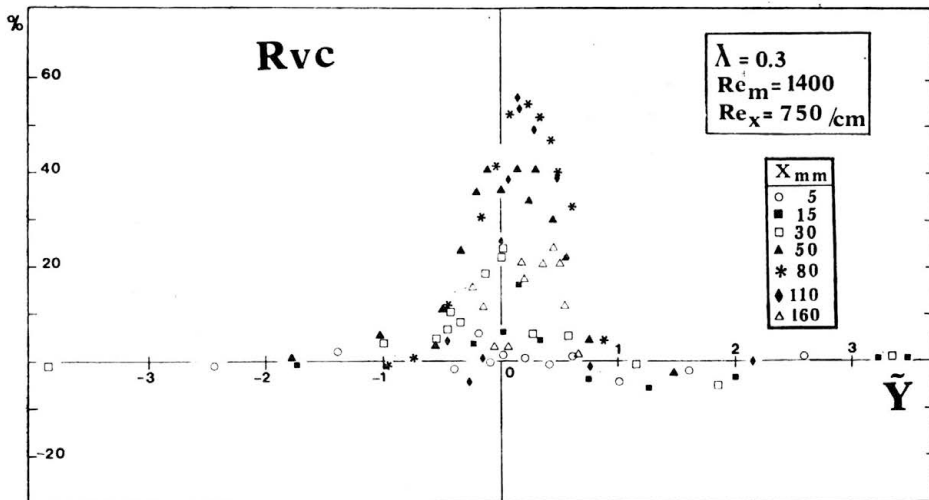FIG. 11. Longitudinal velocity-concentration correlations.

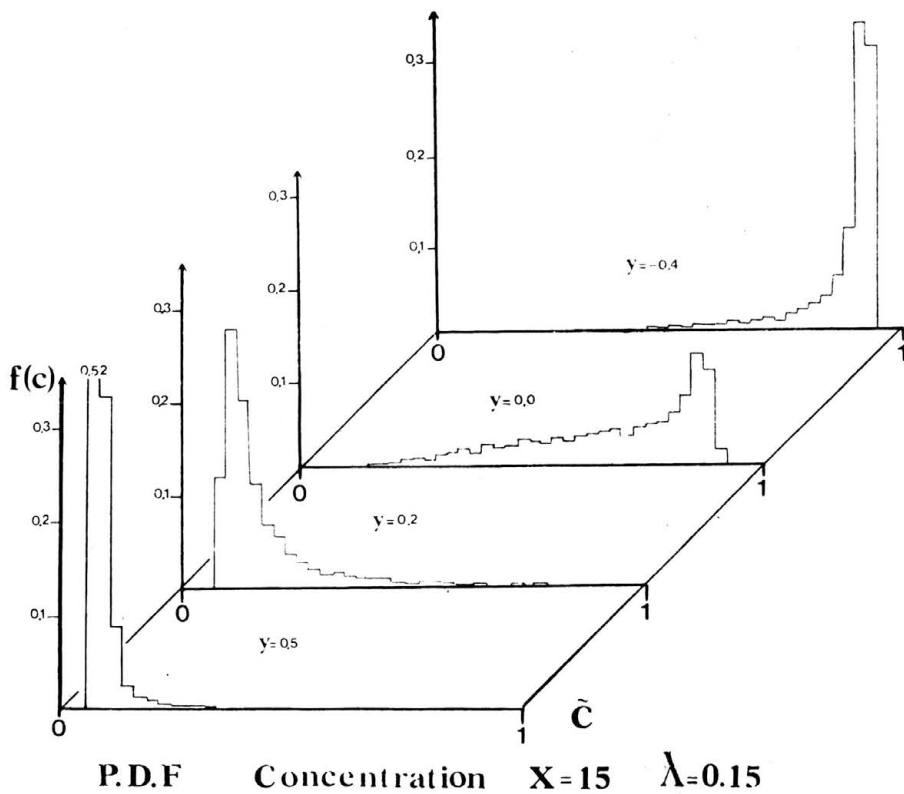FIG. 12. Transverse velocity-concentration correlations.

FIG. 13. Dependence of P.D.F. on y location when $X = 15$ mm.

[429]

the longitudinal structures and the breakup of the two-dimensional vortex have been visualized.

Examination of the probability density function at several stations (Figs. 13, 14 and 15) shows the non-Gaussian behaviour of the concentration distribution. In the region where coherent structures have been found (-2 mm $\leqslant y \leqslant 2$ mm when $X = 8$ cm), the concentration value strongly fluctuates between two distant limits. The bimodal character of the curves corresponds to the crossing of successive packages of pure water and the unmixed potassium chloride solution. Such results show that the mass transport is controlled by the large coherent structures which are characteristic of mixing layers.
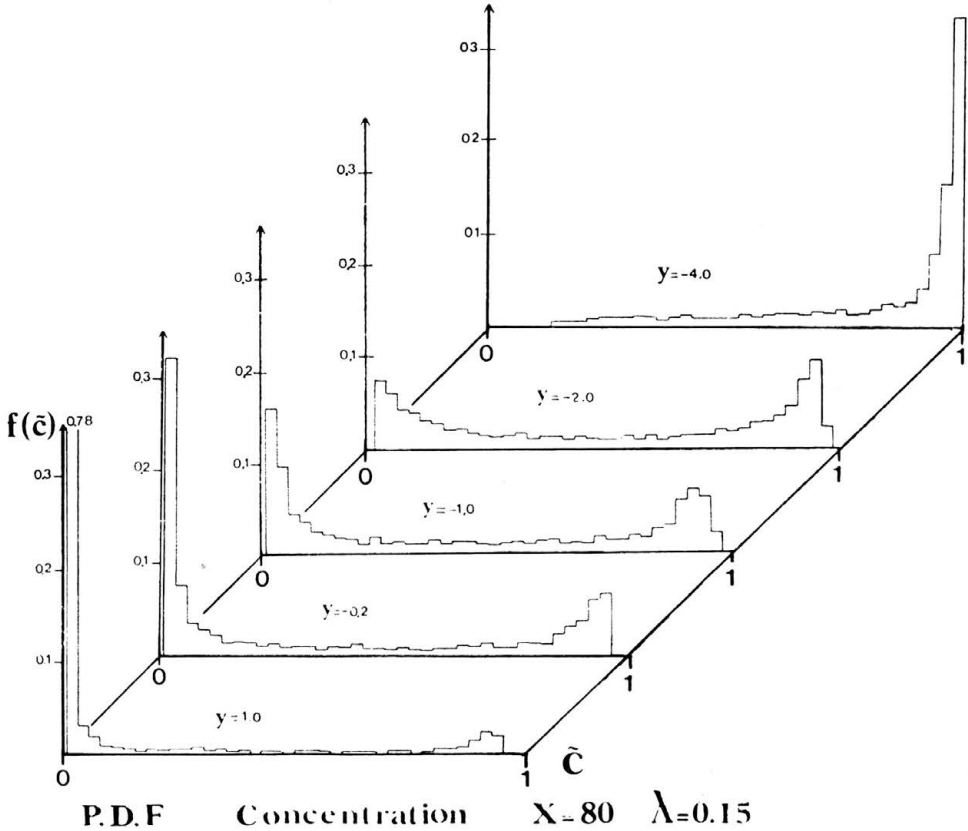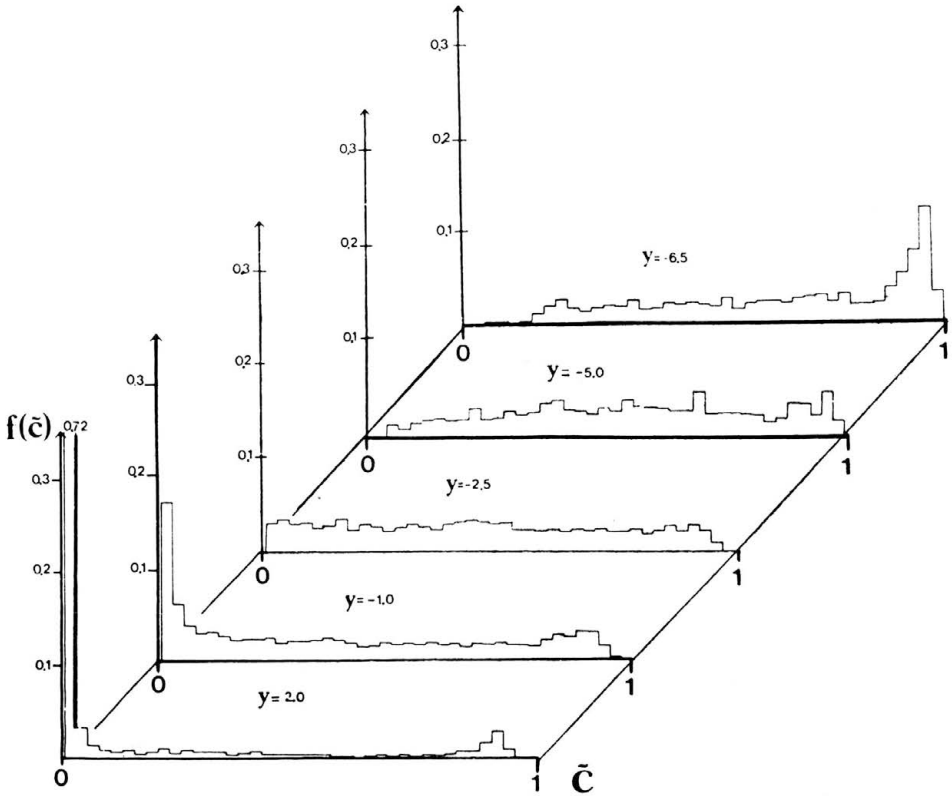

FIG. 14. Dependence of P.D.F. on y location when $X = 80$ mm.

3. Conclusion

Some new results about the flow field and the turbulent transport of a solute substance in a two-dimensional shear layer between liquid streams have been obtained. The appearance the development and the breakup of the large scale two-dimensional vortex are functions of the velocity ratios. These coherent structures control the greater part of the mass transport across the mixing zone as this can be observed from the probability density functions of the diffusing substance obtained in several cross sections of the flow.

FIG. 15. Dependence of P.D.F. on y location when $X = 110$ mm.

References

1. H. E. FIEDLER, Advances in Geophysics, 18a, 93, 1974.
2. C. BEGUIER, L. FULACHIER, J. F. KEFFER, J.F.M., **89**, 3, 561, 1978.
3. R. G. BATT, J. F. M., **82**, 1, 53, 1977.
4. R. S. TORREST, W. E. RANZ, A.ICh.E.J., **16**, 6, 931, 1970.
5. R. E. BREIDENTHAL, A.I.A.A.J., **17**, 3, 310, 1979.
6. J. E. BROADWELL, R. E. BREIDENTHAL, J.F.M., **125**, 397, 1982.
7. J. L. BOUSGARBIES, J. NERAULT, J. M. GATARD, P.C.H., **3**, 2, 113, 1982.
8. C. D. WINANT, F. K. BROWAND, J. F. M., **63**, 2, 237, 1974.
9. G. L. BROWN, A. ROSHKO, J.F.M., **64**, 4, 775, 1974.
10. S. V. SHERIKAR, R. CHEVRAY, *Turbulent shear flows*, 3, 124, Springer Verlag, 1982.
11. R. E. BREIDENTHAL, J.F.M., 109, 1, 1981.
12. J. JIMENEZ, J.F.M., 132, 319, 1983.
13. R. T. PIERREHUMBERT, S. E. WIDNALL, J.F.M., 114, 59, 1982.

LABORATORY OF AERODYNAMICS, POITIERS, FRANCE.